THE JOURNAL OF BIOLOGICAL CHEMISTRY VOL. 290, NO. 33, pp. 20221–20232, August 14, 2015

Induction of Plasmid Conjugation in *Bacillus subtilis* Is Bistable and Driven by a Direct Interaction of a Rap/Phr Quorum-sensing System with a Master Repressor*[S]

Received for publication, May 8, 2015, and in revised form, June 25, 2015 Published, JBC Papers in Press, June 25, 2015, DOI 10.1074/jbc.M115.664110

Thomas C. Rösch[‡§¶] **and Peter L. Graumann**[‡¶1]

From the [‡]*LOEWE Zentrum für synthetische Mikrobiologie (SYNMIKRO), 35043 Marburg, Germany, the* [§]*Spemann Graduate School of Biology and Medicine (SGBM), 79104 Freiburg, Germany, and the* [¶]*Fachbereich für Chemie, Hans-Meerwein Strasse, Universität Marburg, 35043 Marburg, Germany*

Background: Plasmid pLS20 conjugates only during growth of cells.
Results: DNA binding activity of repressor protein Rco is repressed through binding of Rap protein, which is counteracted by a Phr peptide.
Conclusion: Plasmid-encoded Rap and Phr directly restrict the timing of conjugation to exponential growth, leading to bistable expression of conjugation genes.
Significance: A Rap/Phr/repressor system mediates the unusual timing of plasmid conjugation.

Conjugation of plasmid pLS20 from *Bacillus subtilis* is limited to a time window between early and late exponential growth. Genetic evidence has suggested that pLS20-encoded protein Rco_{LS20} represses expression of a large conjugation operon, whereas Rap protein Rap_{LS20} relieves repression. We show that Rap_{LS20} is a true antirepressor protein that forms dimers *in vivo* and *in vitro* and that it directly binds to the repressor protein Rco_{LS20} in a 1:1 stoichiometry. We provide evidence that Rap_{LS20} binds to the helix-turn-helix-containing domain of Rco_{LS20} *in vivo*, probably obstructing DNA binding of Rco_{LS20}, as seen in competitive DNA binding experiments. The activity of Rap_{LS20} in turn is counteracted by the addition of the cognate Phr_{LS20} peptide, which directly binds to the Rap protein and presumably induces a conformational change of the antirepressor. Thus, a Rap protein acts directly as an antirepressor protein during regulation of plasmid conjugation, turning on conjugation, and is counteracted by the Phr_{LS20} peptide, which, by analogy to known Rap/Phr systems, is secreted and taken back up into the cells, mediating cell density-driven regulation. Finally, we show that this switchlike process establishes a population heterogeneity, where up to 30% of the cells induce transcription of the conjugation operon.

Horizontal gene transfer is a central driving force of bacterial genome evolution and plasticity. Beside transformation and transduction, conjugation is the major determinant in the spread of genetic information among bacteria, endowing recipient cells with new traits, such as catabolic pathways, antibiotic resistance, or even virulence (1, 2).

Conjugative elements are either carried on plasmids or maintained in genomes as integrative conjugative elements (ICEs)[2] (2). Transfer of ssDNA occurs via type IV secretion systems (3) and needs to be tightly regulated to minimize the metabolic burden on the host caused by transcription and synthesis of conjugation genes/proteins and the conjugational transfer itself. Therefore, conjugation genes are either kept in a default OFF state and need to be induced by signaling molecules to be switched ON, or conjugation genes are constitutively expressed but limited in their expression in order to not increase the fitness costs of the host. Constitutive systems, such as those of the IncF plasmid family, integrate transcriptional cues of plasmid and host factors as well as environmental stimuli to control the expression of their transfer region. Inducible conjugation systems either rely on sensing of phenolic compounds like the Ti-plasmids from *Agrobacterium tumefaciens* or on quorum-sensing systems using homoserine lactones as signaling molecules in Gram-negative bacteria or signaling peptides in Gram-positive bacteria (4). Among the peptide-regulated systems, regulation of conjugation of the *Enterococci* plasmids pCF10 and pAD1 has been extensively studied. Conjugative transfer of these plasmids is controlled through the ratio of two peptides; a plasmid-encoded peptide (iCF10/iAD1) promotes the inhibitory function of the master regulator (TraA/PrgX) by keeping the conjugation operon in an OFF state, and a chromosomally encoded peptide (cCF10/iAD1) found in many *Enterococci* strains relieves transcriptional repression of the conjugation operon through competitive binding to the master regulator at high concentrations. Thus, in the presence of plasmid-free cells, the conjugation operon is turned ON, whereas at high donor cell densities, the operon is turned OFF. In *Bacillus subtilis*, the quorum-sensing RapI-PhrI module regulates the transfer of the mobile genetic element ICE*Bs*1, which can also be activated by the RecA-dependent SOS response. In contrast

* This work was supported by the Deutsche Forschungsgemeinschaft (DFG), by the Excellence Initiative of the German Research Foundation (GSC-4, Spemann Graduate School), and by the LOEWE Centre for Synthetic Microbiology, SYNMIKRO, in Marburg. The authors declare that they have no conflicts of interest with the contents of this article.
[S] This article contains supplemental Movie S1.
[1] To whom correspondence should be addressed. Tel.: 49-6421-2822210; Fax: 49-6421-2822262; E-mail: peter.graumann@synmikro.uni-marburg.de.

[2] The abbreviations used are: ICE, integrative conjugative element; Bicine, *N*,*N*-bis(2-hydroxyethyl)glycine; qRT-PCR, quantitative RT-PCR.

to PrgX, RapI activates excision and conjugation of ICE*Bs*1 through induction of cleavage of the master regulator ImmR, which is inhibited at high concentrations of PhrI (5).

Rap proteins have been best characterized for their role in the regulation of developmental processes, such as sporulation and competence in *B. subtilis* (6). Phr peptides are secreted and are generally modified; their gene is located downstream of the gene encoding for their cognate Rap protein, which in most cases is a phosphatase. Dephosphorylation of aspartate response regulators prevents the activation of the master regulator of sporulation, Spo0A. Spo0A receives a phosphoryl group through a relay including the response regulator Spo0F, which the Rap protein acts upon. Increasing levels of processed Phr peptides are taken back up into the cells as cell density rises, and during the transition to stationary phase, enough peptide has accumulated to efficiently bind to the Rap protein, displacing it from the response regulator, such that the phosphorelay can proceed toward initiation of sporulation. During competence development, ComP phosphorylates the response regulator ComA in response to high cell density. Phosphorylation of ComA triggers its DNA binding activity, which leads to the expression of several genes, ultimately resulting in the expression of late competence genes. Unlike sporulation-inhibiting Rap proteins, Rap proteins RapF and RapC act on ComA not via inhibition of its function through dephosphorylation, but through allosterically blocking its DNA-binding domain (7–9) and thereby delaying activation of competence genes until a high concentration of the corresponding Phr is reached.

Recently, it was found that a Rap/Phr-like module also plays a role in the regulation of transfer of the conjugative plasmid pLS20 from *B. subtilis* natto (10), which shows an unusual activity for conjugation; whereas ICE*Bs1* becomes active during the transition from exponential growth to stationary phase (11), pLS20 conjugates with some delay after cells have been resuspended into fresh medium and shuts down DNA transfer during late exponential phase, well before cells cease to grow (12). Interestingly, several components of the conjugation machinery of pLS20 assemble and disassemble at a single cell pole or a single site at the lateral membrane, in parallel with conjugation activity (13). How these kinetics are achieved has been hinted at through the identification of a repressor-like protein, Rco_{LS20}, whose deletion results in higher and constitutive conjugation activity, whereas its overproduction leads to a reduction in conjugation efficiency (10). Induction of pLS20 conjugation is also achieved through overexpression of a plasmid-encoded Rap protein, Rap_{LS20}, which may be counteracted by the expression of its cognate peptide Phr_{LS20}, encoded just downstream of the Rap protein-encoding gene. We show that Rco_{LS20}-mediated repression of pLS20 transfer is relieved through direct interaction with Rap_{LS20}, which is blocked in the presence of Phr_{LS20}. Thus, although the Rap-Phr-mediated regulation is similar to already known mechanisms involved in sporulation or competence development, we show that a Rap-Phr quorum-sensing system can also be applied for biotechnological applications needed during ongoing growth.

Materials and Methods

Bacterial Strains, Plasmids, and Strain Construction—Bacterial strains, plasmid, and primers used in this study are listed in Tables 1 and 2. *Escherichia coli* strain DB3.1 was used to propagate *ccdB*-containing plasmids, Mach1 cells were used for construction of plasmids, and Rosetta (DE3) 2 or BL21 (DE3) 2 cells were used for expression of proteins in *E. coli*. *E. coli* and *B. subtilis* cells were grown in LB medium at 30 or 37 °C, supplemented with the appropriate antibiotics at the following final concentrations: 100 μg ml^{-1} ampicillin, 5 or 15 μg ml^{-1} chloramphenicol, (*B. subtilis* or *E. coli*), 10 or 50 μg ml^{-1} kanamycin (*B. subtilis* or *E. coli*), 25 μg ml^{-1} lincomycin, 1 μg ml^{-1} erythromycin, 100 μg ml^{-1} spectinomycin, and 5 μg ml^{-1} phleomycin.

To transfer the deletion of *sigW*, *rsiW*, and the overexpression construct of *rsiW* in the background of the PY79 pLS20*neo* strain, PY79 pLS20*neo* cells were transformed with 0.1–1 μg of chromosomal DNA from the cognate strains listed in Table 1.

To generate a Gateway-accessible vector for *B. subtilis*, the *dest42* cassette containing a *ccdB* gene, a chloramphenicol resistance gene, and the required attachment (*att*) sites were introduced into plasmid pSG1193 (14). The *dest42* cassette was amplified by PCR using primer pair DEST42_KpnI/DEST42_XhoI and plasmid pCGFP (15) as template. The PCR product was digested with KpnI and XhoI and cloned into correspondingly digested pSG1193, creating plasmid pDEST*Bs1*.

All expression plasmids were generated using the Gateway cloning system (Invitrogen). To generate entry clones of *rco*, *rap*, ΔC-*rco*, and ΔN-*rco*, the genes were amplified by PCR using pLS20*neo* as DNA template and primer pairs Rco_FW/Rco+STOP_RV, Rap_FW/Rap_RV, ΔC-Rco_FW/ΔC-Rco_RV, and ΔN-Rco_FW/Rco+STOP_RV. All PCR products were cloned in pENTR-D-TOPO according to the protocol of the manufacturer. To generate the expression plasmids of the individual genes, we used the Gateway LR Clonase II enzyme mix (Invitrogen). All plasmids were sequenced to verify that the genes were integrated in the right orientation.

To generate a transcriptional fusion between the promoter of the conjugation operon (P_c) and a fluorescent reporter gene, the promoter region and the *mcherry* gene were PCR-amplified using primer pairs P_c_FW/P_c_RV and mcherry_FW/mcherry_RV and the templates pLS20 and pSG1164-mcherry. PCR products were digested using BamHI/NheI (P_c) and NheI/EcoRI (*mcherry*) and ligated into the similarly digested pDG1664 plasmid.

Conjugation Assays—Mating experiments were performed as described previously (16) using strain PG300 as a recipient. For induction of *rco* gene expression, xylose was added to the medium at a final concentration of 0.5%. Accordingly, the addition of 1 mM isopropyl 1-thio-β-D-galactopyranoside to the growth medium induced expression of *rsiW*.

Qualitative and Quantitative RT-PCR—Isolation of total RNA, DNase I treatment, and reverse transcription were performed as described previously (16). For the qualitative RT-PCR analysis of the conjugation operon, 1.5 μl of the cDNA reactions, 1.5 μl of the cDNA reactions omitting reverse transcriptase, and 1.5 μl of pLS20*neo* DNA were used in a 30-μl

TABLE 1
Strains and plasmids used in this study

Strain or plasmid	Description[a]	Source/Reference
Strains		
E. coli		
DB 3.1	F$^-$ *mcrA* Δ(*mrr-hsd*RMS-*mcrBC*) Φ80*lac*ZΔM15 Δ*lac*X74 *rec*A1 *ara*Δ139 Δ(*ara-leu*)7697 *gal*U *gal*K *rps*L (*str*^{R}) *end*A1 *nup*G *fhuA*::*IS2*	Invitrogen
Rosetta (DE3) 2	F$^-$ *omp*T *hsdS*$_B$(R$_B^-$ m$_B^-$) *gal dcm* λ(DE3 [*lac*I *lac*UV5-T7 gene 1 ind1 sam7 nin5]) pLysSRARE (*cm*)	Novagen
Mach1	Δ*rec*A1398 *end*A1 *tonA* Φ80Δ*lac*M15 Δ*lac*X74 *hsd*R (r$_K^-$ m$_K^+$)	Invitrogen
BL21 (DE3)	F$^-$ *omp*T *hsd*S$_B$ (R$_B^-$ m$_B^-$) *gal dcm*	Invitrogen
B. subtilis		
PY79 pLS20*neo*		Ref. 13
1012sigW	*sigW*::*bleo*	Gift of T. Wiegert
1012rsiW	*rsiW*::*spec*	Ref. 32
1012clpX	*clpX*::*cm amyE*::P$_{IPTG}$-*rsiW mls*	Ref. 33
TCR16	PY79 pLS20*neo sigW*::*bleo*	This study
TCR17	PY79 pLS20*neo rsiW*::*spec*	This study
TCR18	PY79 pLS20*neo amyE*::P$_{IPTG}$-*rsiW mls*	This study
TCR19	PY79 pLS20*neo amyE*::P$_{xyl}$-rco *spec*	This study
TCR20	PY79 *thrC*::P$_c$-mcherry *mls*	This study
TCR21	PY79 pLS20*neo thrC*::P$_c$-mcherry *mls*	This study
PG300	PY79 P$_{ctc}$::*gfp cm*	Laboratory collection
Plasmids		
pENTR-D-TOPO	*att*L1 *ccdB att*L2 *kan*	Invitrogen
pHGWA	P$_{T7}$-*his$_6$-rfa* cm amp*	Ref. 34
pNDIV	P$_{BAD}$-*divIVA-dest14 amp cm*	Ref. 15
pNGFP	P$_{T7}$-*gfp-dest17 cm*	Ref. 15
pCGFP	P$_{T7}$-*dest42-gfp cm*	Ref. 15
pDEST*Bs1*	P$_{xyl}$-*dest42-yfp spec amp* 5′*amyE* 3′*amyE*	This work
pTCR16	P$_{xyl}$-*rco yfp spec amp* 5′*amyE* 3′*amyE*	This work
pTCR17	pENTR-D-TOPO *rco kan*	This work
pTCR18	pENTR-D-TOPO *rap kan*	This work
pTCR19	pENTR-D-TOPO Δ*C-rco kan*	This work
pTCR20	pENTR-D-TOPO Δ*N-rco kan*	This work
pTCR21	pHGWA P$_{T7}$-*his$_6$-rco amp*	This work
pTCR22	pHGWA P$_{T7}$-*his$_6$-rap amp*	This work
pTCR23	pNGFP P$_{T7}$-*gfp-rap cm*	This work
pTCR24	pNGFP P$_{T7}$-*gfp*-Δ*C-rco cm*	This work
pTCR25	P$_{BAD}$-*divIVA-rap amp*	This work
pTCR26	P$_{BAD}$-*divIVA-rco amp*	This work
pTCR27	P$_{BAD}$-*divIVA*-Δ*C-rco amp*	This work
pTCR28	P$_{BAD}$-*divIVA*-Δ*N-rco amp*	This work
pTCR29	pDG1664 P$_c$-*mcherry mls*	This work

[a] *amp*, ampicillin-resistant; *cm*, chloramphenicol-resistant; *bleo*, phleomycin-resistant; *spec*, spectinomycin-resistant; *mls*, lincomycin-erythromycin-resistant; *kan*/*neo*, kanamycin/neomycin-resistant. rfa*, reading frame cassette A (Invitrogen).

PCR performed with Q5 High Fidelity DNA polymerase and the primers indicated in Fig. 1*A* and listed in Table 2. Quantitative RT-PCRs of *rco* and *virB11* in the corresponding background strains harvested during exponential growth were conducted as indicated previously (16).

Protein Expression and Purification—Rco and Rap$_{LS20}$ were overexpressed as N-terminal His$_6$ tag fusion proteins. Single colonies of freshly transformed Rosetta (DE3) 2 cells were inoculated in LB medium containing ampicillin and grown overnight at 30 °C. The next day, cells were diluted 1:100 in LB medium containing ampicillin and grown to an optical density of 0.4 at 30 °C. Overexpression of Rco and Rap$_{LS20}$ was induced by the addition of 1 and 0.25 mM isopropyl 1-thio-β-D-galactopyranoside, and incubation of cells continued for 3–4 h before cells were harvested by centrifugation (4 °C, 4000 rpm, 20 min). Cells were washed with LEW buffer (50 mM NaH_2PO_4, 300 mM NaCl; 4 °C, 4000 rpm, 20 min) and frozen at −20 °C.

Frozen cells were resuspended in LEW buffer containing Complete Protease Inhibitor Mixture (Roche Applied Science), 1 μg of DNase, and 0.1 mg/ml lysozyme. Cells were homogenized by three passages through a French press cell and centrifuged at 15,000 rpm for 30 min at 4 °C. The lysates were cleared through a 0.45-μm syringe filter (Filtropur S, Sarstedt) and applied to a Ni-TED 2000 column (Macherey-Nagel). The column was washed with 20 column volumes of LEW, and the proteins were eluted in increasing steps of 25 mM imidazole. Fractions containing His$_6$-Rco were pooled and concentrated by ultrafiltration (Vivaspin 20, 5,000 molecular weight cut-off; Sartorius Stedim). The concentrate was further polished by size exclusion chromatography equilibrated in LEW buffer. Fractions containing Rco were concentrated by ultrafiltration. Glycerol was added to a final concentration of 50%, and aliquots were stored at −20 °C.

His$_6$-Rap was identically purified by affinity chromatography as His$_6$-Rco. Fractions containing His$_6$-Rap were concentrated by ultrafiltration (Vivaspin 20, 10,000 molecular weight cut-off; Sartorius Stedim) and further polished by size exclusion chromatography. For EMSA experiments, the size exclusion chromatography column was equilibrated in Buffer A (12 mM HEPES, 4 mM Tris-HCl, 60 mM KCl, 1 mM EDTA, 1 mM EGTA, pH 8.0), and for all other experiments, the column was equilibrated in LEW100 buffer (50 mM NaH_2PO_4, 100 mM NaCl).

Peptide Synthesis—The synthetic pentapeptide Phr$_{LS20}$ (NH_2-QKGMY-COOH) was purchased from GenScript. According to the recommendations of the manufacturer, the peptide was resuspended in H_2O and stored at −20 °C.

Chemical Cross-linking of Rco—Aliquots of 10 μg of Rco were incubated in Buffer B (100 mM Bicine (pH 8), 300 mM NaCl, 1

TABLE 2

Oligonucleotides used in this study

Restriction sites are underlined.

	Oligonucleotide sequence (5′–3′)
RT-PCR analysis	
1_FW	AAGAGCTTCCATACTCTAAAACAT
1_RV	TAAGGATCCTTTCTAACAAGTATTTAGAGAGATCAA
2_FW	TCCGTTGCATTGTCTAACACAC
2_RV	CACCATGACTGAAAAAGATGTTTTAGAGTAT
3_FW	TAAGCATGCCTACATTAGAAGCAGAACACTGC
3_RV	AGCAGCAATAAATCATCAAGCA
4_FW	TAAGCTAGCAAGGAGATTCCTAGGATGGATGAAAAAGCTATTTTAAGTGATGA
4_ RV	TAAGCATGCCTATACCTTTAATTCACCATTCTTCT
5_FW	TAAGGGCCCTGGATTTGAATAAAGGTATTGAAG
5_RV	TTTGATGTAAGCTGATTCATG
6_FW	TAAGGGCCCTCGATTTTAAAGTACCTGAAGAG
6_RV	TAAATCGATCATTTTCTCACCTCGATTTTCT
7_FW	ATCGAATTCTTGGTAAGTGCCAGCTTTGG
7_RV	TAAGGGCCCCAGCCGATAGACGATTTATATACA
8_FW	ACTGGGCCCACACAAAAGATATTCATAGCTG
8_RV	TAATTTTACCTCCATTAAATTGTCG
9_FW	CACCATGAAGAAAAAGGTATATTCGCTAG
9_RV	TCGAATCAACGATAAAGCAG
10_FW	CACCATGCTTGATGGAGCAGTAATG
10_RV	GTTGTGTTGCTCTGAAGTTGC
11_FW	CACCATGGCTGCTACAAAAGCC
11_RV	TTAGATACCCCCACTTTCATTTAG
12_FW	CACCATGCCAGATAATATTGTAGATATGCT
12_RV	AAGCTTTTTGTAAGAGGCTACTAG
13_FW	ATGGAATTCAACTTTACATCAACGAGATACA
13_RV	CAAGCTCATTTTGTTTGCCA
14_FW	CCTATCGATCGAACTAAAAGGACTTGAAAG
14_RV	ATGGAATTCAACTTTACATCAACGAGATACA
15_FW	ACTGGGCCCGTTTTGATAATAAGATTGCTC
15_RV	ATCGTCAGCTTGGCCAATGTAATCTGT
16_FW	ATATATGATTCAAAGTCAGTAAGA
16_RV	AATAAAGTTATTCATACCATGTAAGATCTT
17_FW	ATGGAATTCTTGATCGAATCAACTGTGTATAT
17_RV	ATCTTCTGTGACACTCATCAAGTATAA
18_FW	GAATTCAAATATTTAATGCGCTCAG
18_RV	CTGAAGCAAAGTTTGCAACAC
19_FW	ACTGGGCCCGGATGTATGGTGATCAGC
19_RV	GAGGAATATCTTGTAGAGAATCTGTGATC
20_FW	TCCAATGAAAGCAAAATTTCTTC
20_RV	TCCTTCATTTACTCTGATGAATTC
21_FW	CACCATGCCGGATCTCAACATC
21_RV	CTACCGGCTCTGTTCCATTTC
22_FW	TAACAATGCTTTGAATAATATTCG
22_RV	TTAATGCTGTTCACCAACATAAAA
23_FW	CACCATGATTTTTAAACTAGATCACTATATCAATG
23_RV	GAAAGCTGTTTTTCTCTTTATCAAT
24_FW	ATGATGTGCTGAAGGTCC
24_RV	TTATTGAGTGTTGCAACAAGA
25_FW	TATAGTTCAAAATCCGACTCTACAGTT
25_RV	TCTGATTTCGTTGTTTCTGATACTC
26_FW	TGAGATCAATTATGGAGAAAAATCC
26_RV	AACGAATTCGTTAAAAAGGAAGGTCATCATCACTAAC
27_FW	ATGTTGAATAGAGTAGTTCTAGTAGGA
27_RV	TCCTTATAAAGTTTAATCGGTATTCTT
28_FW	ATGTTGAATAGAGTAGTTCTAGTAGGA
28_RV	GGTAATGGTCAAGGTTCCC
Amplification of genes	
Rco_FW	CACCGTGGGCAATAGAGAGCAAT
Rco +STOP_RV	CTAGTCCTTTTTTAATTTCATGTATTC
ΔC-Rco_FW	CACCGTGGGCAATAGAGAGCAATT
ΔC-Rco_RV	TTATTCTATATTAGGAATGGAGAGCG
ΔN-Rco_FW	CACCATGCTTCAAATAATGGAGTATATAGC
Rap_FW	CACCATGTTGTCCAAAGTAAAAAAAGTACC
Rap_RV	TCATCCTAACGCCTCCGT
DEST42_KpnI	TAAGGTACCACAAGTTTGTACAAAAAAGCTGAA
DEST42_XhoI	TAACTCGAGCACCACTTTGTACAAGAAAGCT
P_c_FW	TAAGGATCCTTATACCACCTCGCAAAATAAA
P_c_RV	TAAGCTAGCCATTTCCTCTCCTCCTAAATTTTCAATCAGTGTAAAGA
mcherry_FW	TAAGCTAGCATGGTGAGCAAGGGC
mcherry_RV	TAAGAATTCTTACTTGTACAGCTCGTCCA
PCR fragments used for electrophoretic mobility shift assays	
P_{UTR}_FW	CACCATGTATGAATACAATAAATGGGG
P_{UTR} _RV	TCAGTTAATAATAAGTTTAGTAAAAACAGG
P_{cds57}_FW	TTTTAGAAATTGTAAGGGAGGC
P_{cds57} _RV	GCCTCCCTTGTTTCCAGTA

TABLE 2 —*continued*

	Oligonucleotide sequence (5′–3′)
P_{cds80}_FW	ACCCAAAACAGCTGCTATT
P_{cds80}_RV	AAAATTTCACCAGTGAGAAAAC
P_{cds82}_FW	ATCATCTTCTCCCCCCAA
P_{cds82}_RV	GAAAAAAACCTCCTTTAATATGGTAA
qRT-PCR analysis	
Rco_qRT-PCR_FW	GGGTTAAGCCAAACACAAGTAGC
Rco_qRT-PCR_RV	CTGCCTGTGTCGGTCTTTTTC
VirB11_qRT-PCR_FW	TGAAGATACGCGGGAAGGAC
VirB11_qRT-PCR_RV	TACCCCAGGAGAAGTAAGCC
RpsJ_qRT-PCR_FW	GCGGTGCACAAATACAAAG
RpsJ_qRT-PCR_RV	TCGCATAAGAGCATCAACAG
SigA_qRT-PCR_FW	GCAACTTCACCTTCTGACCAC
SigA_qRT-PCR_RV	CCGAATCGAAGACGCAATAC

mM DTT) with increasing concentrations of glutardialdehyde. After 15 min at room temperature, the reactions were stopped through the addition of glycine (pH 8) to a final concentration of 140 mM and incubated for 5 min at room temperature. Aliquots were precipitated by acetone and resuspended in 1× SDS loading buffer. Samples were applied to a Tris-glycine PAGE (Nusep) and visualized by silver staining.

EMSA—Fragments P_c and P_{UTR} as well as the upstream regions of *cds57*, *cds80*, and *cds82* were PCR-amplified using Q5 high-fidelity DNA polymerase, pLS20*neo* as template, and the primers indicated in Table 2. For DNA binding reactions, Rco was diluted in Binding Buffer A (12 mM HEPES (pH 8), 4 mM Tris-HCl (pH 8), 60 mM KCl, 1 mM EDTA, 1 mM EGTA, 2.5 mM DTT, and 100 μg/ml BSA) and incubated in Binding Buffer A for 20 min at 37 °C with a 50 nM concentration of the PCR fragments. For competitive DNA binding reactions, the repressor was incubated with the antirepressor Rap_{LS20} and the Phr_{LS20} peptide for 20 min at room temperature prior to the addition of a 50 nM concentrations of fragments X. All reactions were stopped through the addition of DNA loading buffer (TBE, 3% (v/v) glycerol and bromphenol blue) and loaded on 1% agarose gels prepared with 0.5× TBE. Gels were run in the refrigerator for 45 min at 100 V using 0.5× TBE as running buffer and stained with Midori Green Advance (NIPPON Genetics).

Gradient Sedimentation Analysis—Aliquots of 10, 20, and 30 μM Rco were incubated for 30 min on ice in LEW buffer, and 50 μl were layered on top of a 12-ml sucrose gradient (5–20%) prepared in LEW buffer and centrifuged in a Beckmann SW41 rotor for 16 h at 35,000 rpm and 4 °C. 1-ml fractions were sequentially taken up, precipitated by TCA, washed twice with acetone, resuspended in 1× SDS loading buffer, and analyzed by SDS-PAGE.

Size Exclusion Chromatography—20 μM Rap_{LS20}, 40 μM Rco, and 40 μM Phr_{LS20} were incubated or co-incubated for 30 min on ice in LEW200 buffer (50 mM NaH_2PO_4, 200 mM NaCl), centrifuged at 10,000 × *g* for 10 min at 4 °C, and applied to a Superdex 200 10/300 GL column (GE Healthcare). Fractions of 0.5 ml were collected and analyzed by 15% SDS-PAGE.

Fluorescence Microscopy—For the GFP translocation assay in *E. coli* cells, freshly transformed colonies were incubated overnight at 30 °C in LB medium containing 1% glucose and the appropriate antibiotics. The next day, cells were diluted 1:100 in LB medium containing the appropriate antibiotics and grown at 30 °C and 200 rpm. After 2 h of growth, the culture was split, and expression of the DivIVA fusion proteins were induced by adding 0.2% arabinose to one of the growing cultures. Localization of the GFP fusion proteins was examined 60–90 min after induction. For single-cell gene expression analysis of the reporter gene fusion P_c-*mcherry*, cells were grown overnight in selective LB medium, diluted to an OD of 0.05, and grown at 37 °C and 200 rpm in LB medium. The GFP translocation assays shown in Fig. 5 and the time course experiment shown in Fig. 7*A* were performed using a Zeiss Axio Imager AX10 microscope equipped with a 100× objective (Zeiss Plan Fluor 100×, numerical aperture = 1.45) and a CCD camera (Coolsnap HQ^2, Photometrics). Pictures shown in Fig. 6*A* were acquired using a Nikon Eclipse Ti equipped with a 100× objective (CFI Plan Apo Lambda DM 100× oil, numerical aperture = 1.45, Ph3, Nikon) and a CCD camera (DS-Qi1, Nikon). For time lapse microscopy, cells were first grown to OD 0.4 in LB medium, diluted to an OD of 0.01 in minimal medium, and seeded on an agarose pad made with S750 medium containing 0.1% (w/v) glucose, which was placed into a small imaging dish (μDish 35 mm, Ibidi). Growth of cells was followed at 37 °C using a Nikon Eclipse Ti equipped with a motorized stage, a 100× objective (CFI Apo TIRF 100× oil, numerical aperture = 1.49), a thermostage (Tokai Hit), and an EM-CCD camera (ImagEM X2, Hamamatsu). Fluorescence microscopy pictures were processed using ImageJ version 2.0. Single-cell gene expression was measured either by using MicrobeTracker (17), where phase-contrast images were available, or by manually extracting fluorescence values from each cell in ImageJ version 2.0.

Results

Mapping of the Conjugation Operon Encoded by pLS20—To define the transcriptional organization of the conjugation operon present on pLS20, we performed RT-PCR analysis of total RNA from exponentially growing cultures containing pLS20*neo*, using primer pairs to link adjacent genes (Table 2). For every RT-PCR, we included a cDNA synthesis reaction omitting reverse transcriptase to confirm the absence of DNA contamination and a DNA control reaction to verify the specificity of the reactions. In accordance with our previous study (16), we confirmed co-transcription of genes *cds12* (designated as pLS20_014 in the NCBI database) to *cds35* (pLS20_039) and extended the analysis to the regions located down- and upstream. Fig. 1*B* shows that the operon starts at open reading frame *cds3* (pLS20_005), which corresponds to the second RT-

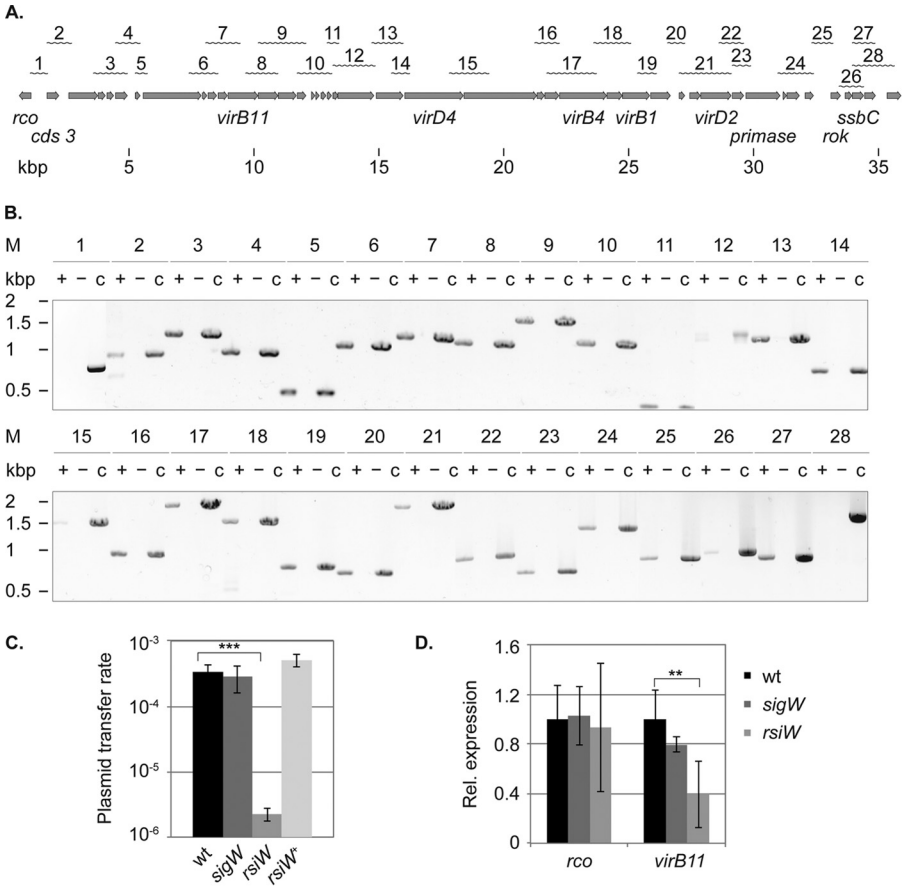

FIGURE 1. **Mapping of the conjugation operon and identification of the promoter driving expression of the *rco* gene.** *A*, physical organization of the operon on the plasmid. *Gray arrows*, individual genes. The *wavy lines* at the *top* indicate the products of the RT-PCR analysis, and the *numbers* correspond to the products shown in *B*. *B*, agarose gel electrophoresis of the RT-PCR analysis. Total RNA was extracted from exponentially growing cultures of PY79/pLS20*neo* and DNase I-digested, and PCRs were performed following cDNA synthesis (+). For every RT-PCR analysis, the product of a cDNA synthesis reaction omitting reverse transcriptase (−) and a PCR with pLS20*neo* DNA as template were included (*c*). *C*, transfer of plasmid pLS20 in strains modulated in the activity of SigW. The plasmid transfer rate is expressed as transconjugants/ml/donor cell and was determined in three independent experiments. *Error bars*, S.D.; statistical significance was calculated using a two-sided independent sample *t* test. ***, $p < 0.001$ compared with the wild type. *D*, quantitative RT-PCR analysis showing transcript levels of *rco* and *virB11* in the background of *sigW* and *rsiW* mutants in relation to the wild type. The *sigA* and *rpsJ* genes served as references for internal normalization. Total RNA was extracted from two independently growing cultures, and qRT-PCRs were conducted in duplicate ($n = 4$). *Error bars*, S.D.; statistical significance was calculated using the Relative Expression Software Tool version 2.0.13 (**, $p < 0.01$).

PCR product of the analysis (Fig. 1*A*), and ends at open reading frame *cds43* (pLS20_049), which corresponds to the second to last RT-PCR product (Fig. 1*A*). Thus, the conjugation operon spans in total more than 33 kbp and also includes genes presumably not involved in the conjugative transfer itself, like *roK* (pLS20_046), the repressor of competence (18), or a putative DNA primase encoded by *cds36* (pLS20_040), which may be required for the establishment of pLS20 in the recipient cell. Our analysis reveals all genes that are up-regulated after cells have been diluted into fresh medium and suggests that their expression is driven by a single promoter region.

Conjugation Is Affected by Enhanced SigW Activity—Rco has been shown to negatively regulate conjugation in *B. subtilis* strain 168 (10). We have found that this is also the case for strain PY79 (data not shown), confirming that the protein acts as a repressor independent of strain background. Ramachandran *et al.* (19) identified two convergent and overlapping promotors that drive the expression of the repressor gene and the conjugation operon. *In silico* analysis of the intergenic region between the first gene of the conjugation operon and the repressor gene using the DBTBS database (20) revealed a *sigW* promoter-like sequence 27 bp upstream of the *rco* gene (5′-cGAAAa-N_{16}-CGTATA). SigW is an extracytoplasmic σ factor, which controls expression of several membrane proteins and which is fully activated upon cell envelope stress (21). It has been shown that the transition state regulator AbrB regulates expression of *sigW* and that transcription of *sigW*-dependent genes increases in a growth phase-dependent manner, with highest expression during stationary phase (21). To test whether the regulatory region of the *rco* gene is a target of SigW, we performed conjugation assays with a *sigW* deletion strain and strains modulating the activity of SigW. Fig. 1*C* shows that the deletion of *sigW* or overexpression of *rsiW*, its cognate anti-σ factor, resulted in slightly higher transfer rates of pLS20. Interestingly, the transfer rate seen in the *rsiW* deletion strain was 2 orders of magnitude lower than that of the wild type strain. Quantitative RT-PCR showed that the relative transcript levels of *rco* and *virB11* as a marker for the conjugation operon were not affected in the background of the *sigW* strain but that deletion of *rsiW* resulted in a lower abundance of *virB11* transcripts (Fig. 1*D*). These experiments reveal a link between SigW activity and transcription of the conjugation operon, which

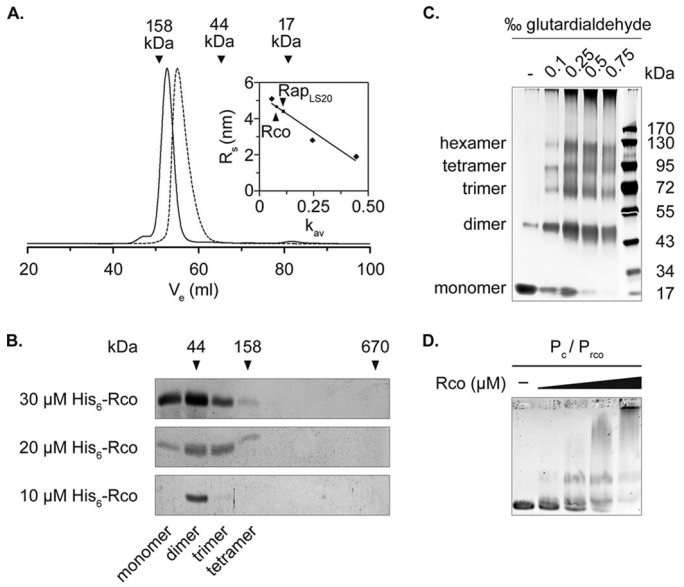

FIGURE 2. **Rco and Rap$_{LS20}$ form dimers in solution.** *A*, size exclusion chromatography of Rco and Rap$_{LS20}$. *Vertical arrows*, elution volumes of the standard proteins used to determine the molecular weight of Rco and Rap$_{LS20}$ (*solid* and *dashed lines*). The *inset* shows the standard curve used for calculating the Stokes radius of Rco (R_S = 4.64) and Rap$_{LS20}$ (R_S = 4.38). Size exclusion chromatography was performed on a HiLoad 16/600 Superdex 75 prep grade column (GE Healthcare). *B*, SDS-PAGE analysis of the 5–20% sucrose gradient sedimentation performed with different concentrations of Rco. Shown are fractions 1–9; *arrows* indicate the sedimentation behavior of the standards run in parallel. The molecular conformations of Rco below the SDS-PAGE analysis were calculated using the Monte-Siegel formula. *C*, chemical cross-linking of Rco with increasing concentrations of glutardialdehyde. Samples were run on 10% Tris-glycine PAGE (Nusep). *D*, binding of His$_6$-Rco to the intergenic region of the repressor gene and the first gene of the conjugation operon containing the promoter of the conjugation operon (P_c) and the repressor gene (P_{rco}). A 50 nM concentration of the DNA fragment was mixed with 0.2, 0.4, 0.8, and 1.6 μM Rco.

does not occur via the transcriptional level of the repressor gene.

Rco and Rap Are Homodimers in Solution, and Rco Binds to Several Sites on the Plasmid—To determine the native weight of the transcriptional regulator and its putative modulator protein, Rap$_{LS20}$, we performed size exclusion chromatography of affinity-purified His$_6$-Rco and His$_6$-Rap$_{LS20}$. Rco eluted at a column volume of 52.6 ml (Fig. 2*A*, *solid line*), which corresponds to a hexameric state of the protein, whereas Rap$_{LS20}$ eluted after 55 ml (Fig. 2*A*, *dashed line*), which corresponds to a dimeric state. Due to the large Stokes radius of Rco (R_S = 4.6) we subsequently performed a sucrose gradient sedimentation analysis of Rco in varying concentrations to further evaluate its oligomeric state. SDS-PAGE analysis and application of the Monte-Siegel analysis combining the Stokes radius and the sedimentation coefficient showed that the repressor mainly exists as a dimer in solution (Fig. 2*B*). At higher concentrations, the repressor was also found to be in trimeric and tetrameric forms. Calculation of the S_{max}/S ratio shows that the monomeric conformation probably represents the most elongated shape, whereas the oligomeric conformations have moderately elongated shapes compared with proteins of known structure. Finally, glutardialdehyde cross-linking experiments confirmed the observation that Rco mainly exists in a dimeric conformation (Fig. 2*C*). Dimer formation was even present without the addition of the cross-linking agent. In its presence, the protein was also seen as trimer, tetramer, and hexamer.

Previous work has shown that Rco regulates transcription of the conjugation operon through binding to two operator sites within the intergenic region of *rco* and the first gene of the conjugation operon, possibly by forming a DNA loop of 75 bp (19). Although we did not observe a preference of the repressor to form tetramers as stated before, we found a DNA binding behavior comparable with that described in the literature (Fig. 2*D*). Specifically, Rco binds with high affinity to sequences containing 5′-CAGTGAAA-3′, which we confirmed using EMSAs and a 125-bp fragment containing an identical sequence, which is located 175 bp upstream of the first gene of the conjugation operon (named P_{UTR}; Fig. 3, *first panel*). However, binding affinity was lower in this region compared with binding to the previously described operator binding sites (19) (Fig. 2*D*), suggesting that the newly identified binding region may act as a secondary repressor binding site.

We wondered if Rco might regulate the expression of other pLS20-encoded genes, and we performed EMSA experiments with the regulatory regions of genes, which were shown to be differently regulated in the background of Rco- or Rap$_{LS20}$-overexpressing strains, as indicated by RNA sequencing analysis of Meijer and co-workers (10). We found that Rco bound to the promoter region of *cds80* (pLS20_102; Fig. 3, *second panel*), a protein of unknown function with a predicted signal peptide sequence, but not to regions preceding gene *cds57* (pLS20_101) and the putative operon of *cds81* and *cds82* (pLS20_105 and pLS20_106). Similar to fragment P_{UTR}, the region upstream of *cds80* contains a conserved consensus sequence, which differs only in 1 base (5′-CAGTGAgA-3′) from the sequence shown to be the consensus binding site of Rco. Nevertheless, it seems that additional purine residues at the 3′-end of the consensus sequence increase the binding affinity of the repressor. These experiments show that Rco binds to several sites in the conjugation promoter region and to at least one additional site on the plasmid.

Rap$_{LS20}$ Binds Directly to Rco to Inhibit Its DNA Binding Activity, whereas the Addition of Phr$_{LS20}$ Relieves the Inhibitory Function of Rap$_{LS20}$ on Rco—Genetic evidence has shown that an endogenous Rap-Phr module on pLS20 (Rap$_{LS20}$ and Phr$_{LS20}$) affects the activity of the repressor of conjugation (10). To determine whether Rap$_{LS20}$ directly regulates the activity of the repressor protein through protein-protein interactions, we performed analytical size exclusion chromatography of Rap$_{LS20}$, Rco, and a mixture of both proteins. Fig. 4*A* shows that Rap$_{LS20}$ eluted much earlier from the column upon the addition of Rco than alone, providing evidence for complex formation of these proteins. The complex migrated at a molecular mass of 154 kDa, suggesting the formation of a heterotetrameric complex ((2 × 46.6 kDa) + (2 × 21.8 kDa)) with a 1:1 stoichiometry, as determined by densitometric measurements of the corresponding bands.

It is known that the function of Rap proteins is controlled by their cognate Phr peptides through protein-peptide interactions (6, 22). Meijer and co-workers (10) showed that the 5 C-terminal residues of the Phr$_{LS20}$ prepeptide (corresponding to QKGMY) efficiently repressed conjugation of plasmid pLS20

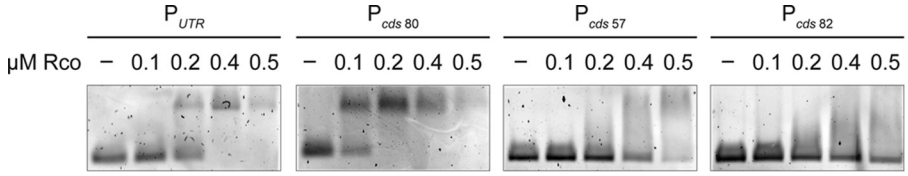

FIGURE 3. **Identification of additional binding sites of the Rco repressor.** Rco additionally binds to DNA fragments immediately upstream of the first gene of the conjugation operon (fragment P_{UTR}) and upstream of gene *cds80* (*first* and *second panels*) but not to upstream regions of *cds57* and *cds82* (*third* and *fourth panels*). Increasing concentrations of isolated Rco were incubated with 50 nM DNA.

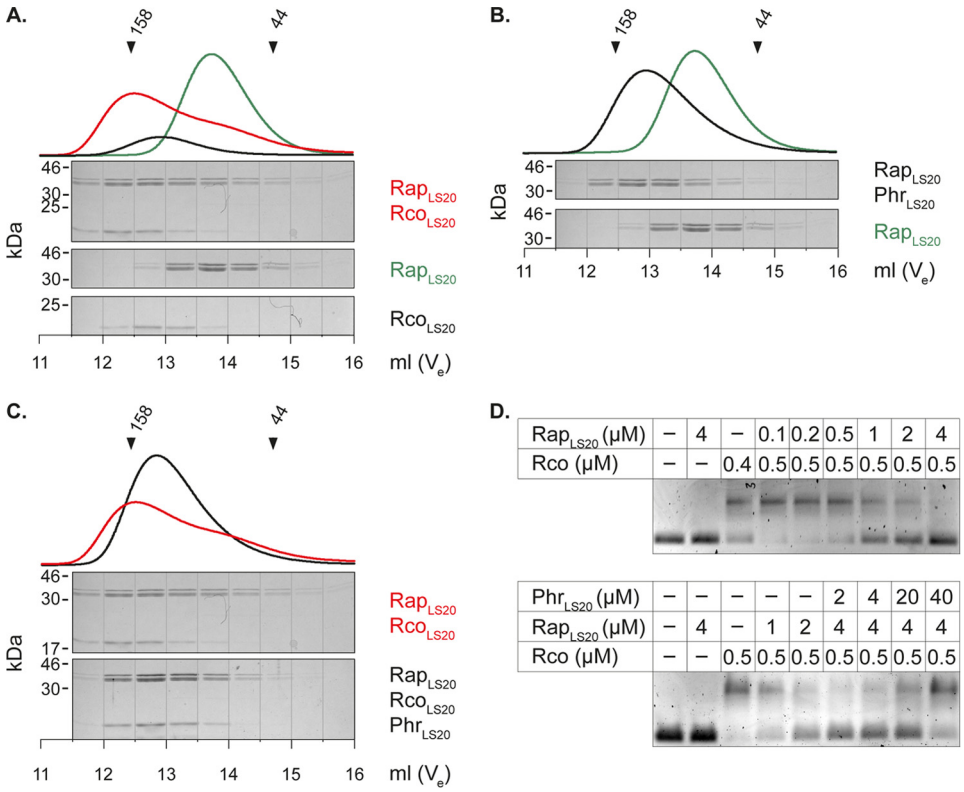

FIGURE 4. **Rap_{LS20} binds to Rco and inhibits the DNA binding activity of Rco, whereas Phr_{LS20} relieves the inhibitory effect of Rap_{LS20}.** *A*, *in vitro* interaction of Rap_{LS20} and Rco. Size exclusion chromatography of Rap_{LS20} (20 μM), Rco (40 μM), and Rap_{LS20}-Rco in complex (20 and 40 μM) was performed on a Superdex 200 10/300 GL column. *Top*, chromatograms; *bottom*, SDS-PAGE analysis of the eluted fractions. *B*, Phr_{LS20} binds to Rap_{LS20}. The addition of 40 μM Phr_{LS20} to 20 μM Rap_{LS20} changes the elution profile of Rap_{LS20}. *C*, the addition of 40 μM Phr_{LS20} disrupts complex formation of Rap_{LS20} and Rco (20 and 40 μM). *D*, *top*, Rap_{LS20} inhibits DNA binding activity of Rco; *bottom*, Phr_{LS20} relieves the inhibitory effect of Rap_{LS20} on DNA binding activity of Rco. Rco was mixed with Rap_{LS20} and Phr_{LS20} at the indicated concentrations prior to the addition of 50 nM P_{UTR}.

and that repression could be relieved by deletion of the oligopeptide permease *opp*.

To verify that Phr_{LS20} acts on Rap_{LS20}, thereby possibly interfering with complex formation of Rap_{LS20}-Rco, we added the synthetic pentapeptide to Rap_{LS20} and to Rap_{LS20}-Rco complexes. Indeed, synthetic Phr_{LS20} bound to Rap_{LS20}, causing Rap_{LS20} to elute earlier from the column (Fig. 4*B*) than when in complex with Rco. Additionally, co-incubation of Phr_{LS20} with Rap_{LS20} and Rco prevented complex formation between the two proteins (Fig. 4*C*), at the expense of the Rap_{LS20}-Phr_{LS20} complex.

To test whether an interaction between Rap_{LS20} and Rco results in an inhibition of the DNA binding activity of the repressor protein, we conducted EMSA experiments in the presence of increasing amounts of Rap_{LS20}. As indicated in Fig. 4*D*, Rap_{LS20} showed no DNA binding activity by itself but diminished the binding activity of Rco when the molar ratio reached a 1:1 stoichiometry and completely repressed DNA binding at an 8-fold molar excess (Fig. 4*D*, *top*). To see whether Phr_{LS20} relieves the inhibitory function of Rap_{LS20} on Rco, we added increasing amounts of Phr_{LS20} to the (8-fold) molar ratio of Rap_{LS20} and Rco at which no more DNA binding activity occurred. Interestingly, the addition of the peptide restored the DNA binding activity of Rco, although not to the same extent as without the addition of Rap_{LS20} (Fig. 4*D*). These results show that the Rco/Rap_{LS20}/Phr_{LS20} module on pLS20 operates via direct protein-protein and protein-peptide interactions to regulate the conjugative activity of the plasmid.

Rap_{LS20} Interferes with Rco Function through Interaction with the N Terminus of Rco—Previous studies revealed that RapF prevents binding of ComA to its target promoters by blocking the DNA-binding domain of ComA through a direct interaction (7, 8). We wondered whether this might be a general scheme of Rap proteins that regulate the activity of transcriptional regulators. To shed light on the interaction interface of Rap_{LS20} and Rco, we applied an *in vivo* GFP translocation assay

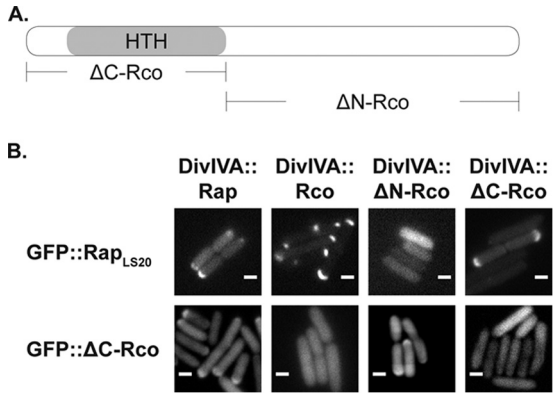

FIGURE 5. **Rap$_{LS20}$ interacts with the N terminus of the repressor containing the DNA binding motif.** *A*, graphical representation of the repressor protein and its derivatives used for the translocation assay. *B*, *top*, heterologous co-expression of GFP::Rap$_{LS20}$ with DivIVA fusions of Rap$_{LS20}$, Rco, and C- or N-terminally truncated versions of Rco. *Bottom*, heterologous co-expression of GFP::ΔC-Rco with DivIVA fusions of Rap$_{LS20}$, Rco, and C- or N-terminally truncated versions of Rco. *Scale bar*, 2 μm.

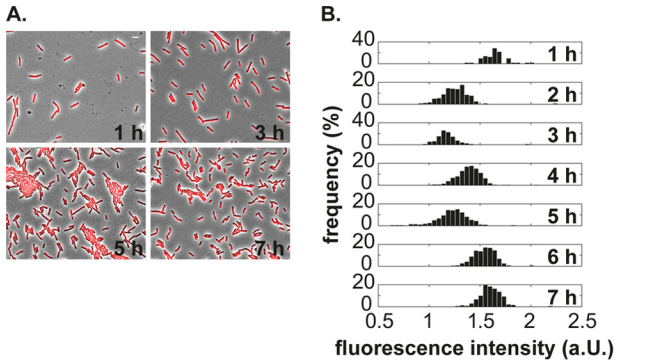

FIGURE 6. **Cells devoid of the plasmid show a homogeneous expression of the promoter of conjugation when ectopically integrated into the chromosome of *B. subtilis*.** *A*, fluorescence pictures of PY79 cells carrying P$_c$-*mcherry*. Shown are overlays of fluorescent and phase-contrast images taken at the indicated time points. *Scale bar*, 4 μm. *B*, cells devoid of the plasmid exhibit a unimodal distribution of the fluorescent signal. Shown are log-transformed signal intensities plotted on a linear scale. *a.U.*, arbitrary units.

based on the intrinsic property of DivIVA to localize at negative membrane curvatures (23, 24). Therefore, we fused Rap$_{LS20}$ to GFP and co-expressed it pairwise with DivIVA fusions to full-length Rco or with DivIVA fusions to the C- or the N-terminal ends of Rco (ΔC-Rco and ΔN-Rco; Fig. 5*A*) in *E. coli* BL21 (DE3) cells. In all cases, we observed strong GFP signals even in the absence of the inducing agent (isopropyl 1-thio-β-D-galactopyranoside); thus, we split the cultures before induction of the DivIVA fusion proteins to clearly distinguish DivIVA-like localization from polar localization caused by overexpression of the GFP fusion proteins.

We found that GFP-Rap$_{LS20}$ localized in a half-moon-like manner to the cell pole when co-expressed with a DivIVA fusion of Rap$_{LS20}$, of full-length Rco, or of ΔC-Rco, but not when it was co-expressed with a DivIVA fusion of ΔN-Rco (Fig. 5*B*, *top*). To test whether these proteins indeed interact via the N terminus of Rco, we also assayed the localization of GFP-ΔC-Rco only containing the helix-turn-helix motif upon co-expression with DivIVA-Rap$_{LS20}$. As shown in Fig. 5*B* (*bottom*), DivIVA-Rap$_{LS20}$ targeted GFP-ΔC-Rco to the cell pole and to a certain extent also DivIVA-ΔN-Rco, but no translocation was observed when GFP-ΔC-Rco was co-expressed with DivIVA-Rco or with DivIVA-ΔC-Rco. Taken together, we provide evidence that Rap$_{LS20}$ recognizes the N-terminal part of Rco containing the helix-turn-helix motif.

Expression of the Conjugation Operon is Heterogeneous—To test whether, during growth, all cells or just a subset induce the conjugation operon, as is often characteristic of developmental pathways in bacteria, we monitored the activity of the promoter driving expression of the large conjugation operon at the single cell level. Therefore, we generated a transcriptional fusion of the promoter (P$_c$) with the fluorescent mCherry protein and integrated the reporter gene fusion into the *thrC* locus in the chromosome of *B. subtilis* PY79. First, we analyzed its expression during growth in cells devoid of the plasmid and its regulatory elements. Signal intensities of the fluorescent reporter were homogeneously distributed during all growth stages in cells lacking the plasmid (Fig. 6, *A* and *B*), although the mean fluorescence intensity varied between the time points (Fig. 6*B*).

Contrary to plasmid-free cells, cells containing the plasmid exhibited a phenotypic heterogeneity in the expression pattern of the fluorescent reporter (Fig. 7*A*, *red* and *white arrows*). To quantitatively analyze expression of the promoter of conjugation, we measured the mCherry fluorescence signal of individual cells at each time point during growth and plotted the log-transformed fluorescence intensities in histograms. Fig. 7*B* shows that the overall signal intensity increases with ongoing growth and that the fluorescence intensity shifts from a rather unimodal distribution to a bimodal distribution upon entry into mid-exponential growth (*first* and *second panel* from the *top*). Similarly, after 8 h of growth, the fluorescence intensity shifted back to a unimodal distribution. To determine the number of cells switching on the conjugation operon, we set a threshold that separated the two populations from each other and calculated the number of cells exceeding the intensity threshold (Fig. 7*B*). Fig. 7*C* shows that under our conditions, a maximum of about 30% of the cells switched the operon to the ON state during the transition from the lag phase to exponential phase of growth. To further analyze the phenotypic heterogeneity of the promoter of conjugation at the single cell level, we performed time lapse microscopy. In accordance with the previous time course experiment, we observed two distinct populations. Additionally, we found that once induced, expression of the conjugation promoter was stably inherited in dividing cells and slowly disappeared when cells ceased to divide (Fig. 7*D* and supplemental Movie S1). These experiments reveal that the Rap/Phr/repressor system on pLS20 operates in a bistable manner, similar to the ComS/MecA/ComK system in competence and to the phosphorelay in sporulation. Our findings extend the previous observation that only a subset of cells assemble the conserved type IV secretion proteins at the membrane (13) and provide evidence that the assembly of the type IV secretion is already regulated at the transcriptional level.

Discussion

Rap-Phr modules play a pivotal role in determining the fate of individual cells in bacterial communities and are best characterized in *B. subtilis* (22, 25). So far, several modules in the

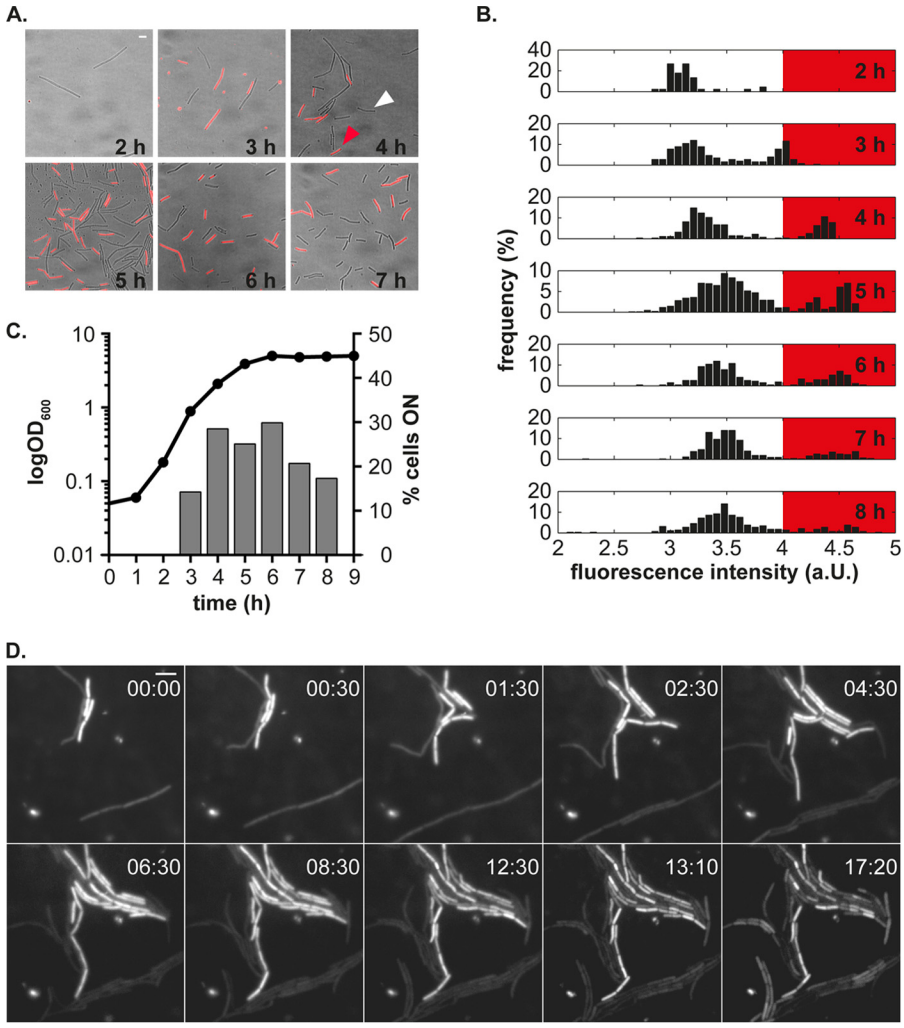

FIGURE 7. **Phenotypic heterogeneity of the conjugation operon during growth of *B. subtilis*.** *A*, the promoter of conjugation shows a heterogonous expression pattern in the presence of regulatory elements encoded by plasmid pLS20. Fluorescence microscopy pictures were overlaid on bright field microscopy pictures to indicate the coexistence of two states in the clonal population of pLS20-containing cells carrying a P_c-*mcherry* fusion. *Scale bar*, 4 μm. *B*, fluorescence distribution of the mCherry reporter protein under control of the promoter of conjugation (P_c) at different time points during growth. Histograms derived from the time course experiment show a bimodal distribution. The *red box* highlights the signal intensities above the threshold used to calculate the number of cells switching the conjugation operon to the ON state. Fluorescence intensities were log-transformed and plotted linearly. *C*, percentage of cells exceeding the fluorescence threshold during growth. *Left y axis*, growth of cells; *right* y *axis*, number of cells expressing the fluorescent reporter protein above the threshold. *D*, snapshots from a representative time lapse experiment illustrate the stable expression of the fluorescent reporter protein mCherry from the P_c promoter during microcolony development. The time scale is represented in hours, and the *scale bar* corresponds to 4 μm. *a.U.*, arbitrary units.

genome of *B. subtilis* have been discovered that affect sporulation, competence development, secretion of extracellular proteases, or the horizontal transfer of the mobile genetic element ICE*Bs*1. In this work, we provide *in vitro* and *in vivo* evidence that the Rap/Phr module on conjugative plasmid pLS20 directly regulates conjugation via binding to the Rco master repressor and that induction of conjugation occurs in a bistable manner, similar to the developmental processes of competence development and sporulation, leading to heterogeneous expression of the type IV secretion machinery encoded on pLS20. We show that Rap_{LS20} acts as a direct antirepressor of the Rco protein and that its activity is regulated by the cognate Phr_{LS20} peptide. We show that the repressor and its antirepressor preferentially form dimers in solution and that complex formation occurs in a 1:1 stoichiometry that disrupts DNA binding of the repressor protein through obscuring the DNA-binding domain of the repressor. Unlike the plasmid-encoded Rap60, which presumably inactivates ComA activity by occluding its interaction with the RNA polymerase (26), inactivation of the Rco repressor by Rap_{LS20} resembles that of RapC, -F, and -H, which prevent DNA binding of ComA, which, however, is an activator, rather than a repressor, like Rco. Structural analysis of the RapF-ComA interaction showed that the N-terminal 3-helix bundle of RapF captures the helix-turn-helix-containing domain of ComA and thereby prevents binding of ComA to its target promoters (8). Concurrent with its different binding partner, Rap_{LS20} shows substitutions in all amino acid residues shown to be essential for the interaction of RapF and ComA (8).

Recent work showed that high levels of Phr peptide inhibit horizontal transfer of the plasmid, whereas at lower levels, the Rap protein becomes active and switches on the expression of the conjugation operon (10). Therefore, the known *in vivo* data nicely corroborate our *in vitro* findings.

Interestingly, several plasmids, such as pBS32 of the undomesticated *B. subtilis* strain NCIB3610, pX01 of *Bacillus anthracis*, and pTA1060 of *B. subtilis* were found to carry Rap/Phr modules known to affect the developmental fate of their host (27–29), showing that the use of Rap/Phr modules is widespread.

The interaction of RapF-ComA is antagonized through binding of PhrF to the C-terminal tetratricopeptide repeat domain of RapF. In the PhrF-bound state, RapF constricts and exerts a conformational change that leads to dissociation of the RapF-ComA complex (30, 31). Phr_{LS20} seems to induce a conformational change in Rap_{LS20} as well, but our size exclusion chromatography data indicate that Rap_{LS20} rather elongates or expands upon binding to the peptide, because the protein-peptide complex is much larger than Rap_{LS20} alone. In fact, although Rap proteins share a high degree of overall sequence homology, it was not possible to model the structure of Rap_{LS20} based on the previously solved structures. Thus, it would be interesting to reveal how the structures of Rap_{LS20} and Rap_{LS20}-Phr_{LS20} differ from already known structures.

Furthermore, we show that Rco also binds to a second promoter region on the plasmid, suggesting that it regulates at least two transcriptional units. Interestingly, we found that increased activity of SigW through deletion of its antagonist RsiW resulted in a diminished plasmid transfer rate, whereas expression of the *rco* gene was not significantly affected in the background of these strains. Nevertheless, we found that expression of *virB11* was slightly but significantly changed in the *rsiW* strain. Due to the only moderate effect, we think that the reduced plasmid transfer rate seen in the *rsiW* strain is probably due to secondary effects caused by enhanced SigW activity and not by direct transcriptional regulation of the repressor gene or the conjugation operon. In any event, it is intriguing to note that changes in the activity of a host-encoded σ factor affect conjugation activity of a plasmid, which may be important for the plasmid's decision to prevent conjugation in case of existing cell wall stress.

Last, we provide evidence that expression of the conjugation operon occurs in a heterogeneous but stable manner. Whereas in the absence of the plasmid, expression of the ectopic conjugation promoter showed a unimodal distribution, the presence of the plasmid elicited a bimodal distribution and thus a mutually exclusive expression pattern of the conjugation promoter in the population. Interestingly, time lapse microscopy revealed that once the ON state is established, expression of the conjugation promoter is propagated to the next generation of cells and vanishes with additional cell divisions. Interestingly, the Meijer group (19) recently showed that repressor protein Rco_{LS20} autoregulates itself and keeps the conjugation operon in the OFF state through binding to two operator sites, presumably forming a DNA loop. Loop formation may contribute to the relatively tight on/off regulation seen in our expression studies.

Our work shows that pLS20 harbors a classical Rap/Phr system, which modulates the activity of a repressor protein, but its output *in vivo* differs from known Rap/Phr systems, in that the partner switch shows an offset *in vivo* relative to known Rap/Phr systems as it occurs during a time window, when cells actively divide rather than arrest their cell cycle. Thus, the Rco/Rap/Phr regulatory circuit encoded by plasmid pLS20 could be employed for the rational design of expression systems that are limited to the cell's growth phase. It will be interesting to further analyze which factor(s) governs the heterogeneous expression of the conjugation operon.

Author Contributions—T. C. R. and P. L. G. conceived of and coordinated the study and wrote the paper. T. C. R. designed, performed, and analyzed the experiments. All authors reviewed the results and approved the final version of the manuscript.

Acknowledgment—We thank Thomas Wiegert (University of Zittau, Germany) for the generous gift of the sigW mutant strain.

References

1. Chen, I., Christie, P. J., and Dubnau, D. (2005) The ins and outs of DNA transfer in bacteria. *Science* **310,** 1456–1460
2. Thomas, C. M., and Nielsen, K. M. (2005) Mechanisms of, and barriers to, horizontal gene transfer between bacteria. *Nat. Rev. Microbiol.* **3,** 711–721
3. Christie, P. J., Atmakuri, K., Krishnamoorthy, V., Jakubowski, S., and Cascales, E. (2005) Biogenesis, architecture, and function of bacterial type IV secretion systems. *Annu. Rev. Microbiol.* **59,** 451–485
4. Grohmann, E., Muth, G., and Espinosa, M. (2003) Conjugative plasmid transfer in Gram-positive bacteria. *Microbiol. Mol. Biol. Rev.* **67,** 277–301
5. Bose, B., and Grossman, A. D. (2011) Regulation of horizontal gene transfer in *Bacillus subtilis* by activation of a conserved site-specific protease. *J. Bacteriol.* **193,** 22–29
6. Perego, M., and Brannigan, J. A. (2001) Pentapeptide regulation of aspartyl-phosphate phosphatases. *Peptides* **22,** 1541–1547
7. Bongiorni, C., Ishikawa, S., Stephenson, S., Ogasawara, N., and Perego, M. (2005) Synergistic regulation of competence development in *Bacillus subtilis* by two Rap-Phr systems. *J. Bacteriol.* **187,** 4353–4361
8. Baker, M. D., and Neiditch, M. B. (2011) Structural basis of response regulator inhibition by a bacterial anti-activator protein. *PLoS Biol.* **9,** e1001226
9. Core, L., and Perego, M. (2003) TPR-mediated interaction of RapC with ComA inhibits response regulator-DNA binding for competence development in *Bacillus subtilis*. *Mol. Microbiol.* **49,** 1509–1522
10. Singh, P. K., Ramachandran, G., Ramos-Ruiz, R., Peiró-Pastor, R., Abia, D., Wu, L. J., and Meijer, W. J. (2013) Mobility of the native *Bacillus subtilis* conjugative plasmid pLS20 is regulated by intercellular signaling. *PLoS Genet.* **9,** e1003892
11. Auchtung, J. M., Lee, C. A., Monson, R. E., Lehman, A. P., and Grossman, A. D. (2005) Regulation of a *Bacillus subtilis* mobile genetic element by intercellular signaling and the global DNA damage response. *Proc. Natl. Acad. Sci. U.S.A.* **102,** 12554–12559
12. Itaya, M., Sakaya, N., Matsunaga, S., Fujita, K., and Kaneko, S. (2006) Conjugational transfer kinetics of pLS20 between *Bacillus subtilis* in liquid medium. *Biosci. Biotechnol. Biochem.* **70,** 740–742
13. Bauer, T., Rösch, T., Itaya, M., and Graumann, P. L. (2011) Localization pattern of conjugation machinery in a Gram-positive bacterium. *J. Bacteriol.* **193,** 6244–6256
14. Feucht, A., and Lewis, P. J. (2001) Improved plasmid vectors for the production of multiple fluorescent protein fusions in *Bacillus subtilis*. *Gene* **264,** 289–297
15. Edwards, A. N., Fowlkes, J. D., Owens, E. T., Standaert, R. F., Pelletier, D. A., Hurst, G. B., Doktycz, M. J., and Morrell-Falvey, J. L. (2009) An *in vivo* imaging-based assay for detecting protein interactions over a wide range of binding affinities. *Anal. Biochem.* **395,** 166–177
16. Rösch, T. C., Golman, W., Hucklesby, L., Gonzalez-Pastor, J. E., and Graumann, P. L. (2014) The presence of conjugative plasmid pLS20 affects global transcription of its *Bacillus subtilis* host and confers beneficial stress resistance to cells. *Appl. Environ. Microbiol.* **80,** 1349–1358
17. Sliusarenko, O., Heinritz, J., Emonet, T., and Jacobs-Wagner, C. (2011)

High-throughput, subpixel precision analysis of bacterial morphogenesis and intracellular spatio-temporal dynamics. *Mol. Microbiol.* **80,** 612–627
18. Singh, P. K., Ramachandran, G., Durán-Alcalde, L., Alonso, C., Wu, L. J., and Meijer, W. J. (2012) Inhibition of *Bacillus subtilis* natural competence by a native, conjugative plasmid-encoded comK repressor protein. *Environ. Microbiol.* **14,** 2812–2825
19. Ramachandran, G., Singh, P. K., Luque-Ortega, J. R., Yuste, L., Alfonso, C., Rojo, F., Wu, L. J., and Meijer, W. J. (2014) A complex genetic switch involving overlapping divergent promoters and DNA looping regulates expression of conjugation genes of a Gram-positive plasmid. *PLoS Genet.* **10,** e1004733
20. Sierro, N., Makita, Y., de Hoon, M., and Nakai, K. (2008) DBTBS: a database of transcriptional regulation in *Bacillus subtilis* containing upstream intergenic conservation information. *Nucleic Acids Res.* **36,** D93–D96
21. Cao, M., Wang, T., Ye, R., and Helmann, J. D. (2002) Antibiotics that inhibit cell wall biosynthesis induce expression of the *Bacillus subtilis* σ(W) and σ(M) regulons. *Mol. Microbiol.* **45,** 1267–1276
22. Perego, M. (2013) Forty years in the making: understanding the molecular mechanism of peptide regulation in bacterial development. *PLoS Biol.* **11,** e1001516
23. Lenarcic, R., Halbedel, S., Visser, L., Shaw, M., Wu, L. J., Errington, J., Marenduzzo, D., and Hamoen, L. W. (2009) Localisation of DivIVA by targeting to negatively curved membranes. *EMBO J.* **28,** 2272–2282
24. Ramamurthi, K. S., and Losick, R. (2009) Negative membrane curvature as a cue for subcellular localization of a bacterial protein. *Proc. Natl. Acad. Sci. U.S.A.* **106,** 13541–13545
25. Schultz, D., Wolynes, P. G., Ben Jacob, E., and Onuchic, J. N. (2009) Deciding fate in adverse times: sporulation and competence in *Bacillus subtilis*. *Proc. Natl. Acad. Sci. U.S.A.* **106,** 21027–21034
26. Boguslawski, K. M., Hill, P. A., and Griffith, K. L. (2015) Novel mechanisms of controlling the activities of the transcription factors Spo0A and ComA by the plasmid-encoded quorum sensing regulators Rap60-Phr60 in *Bacillus subtilis*. *Mol. Microbiol.* **96,** 325–348
27. Bongiorni, C., Stoessel, R., Shoemaker, D., and Perego, M. (2006) Rap phosphatase of virulence plasmid pXO1 inhibits *Bacillus anthracis* sporulation. *J. Bacteriol.* **188,** 487–498
28. Parashar, V., Konkol, M. A., Kearns, D. B., and Neiditch, M. B. (2013) A plasmid-encoded phosphatase regulates *Bacillus subtilis* biofilm architecture, sporulation, and genetic competence. *J. Bacteriol.* **195,** 2437–2448
29. Koetje, E. J., Hajdo-Milasinovic, A., Kiewiet, R., Bron, S., and Tjalsma, H. (2003) A plasmid-borne Rap-Phr system of *Bacillus subtilis* can mediate cell-density controlled production of extracellular proteases. *Microbiology* **149,** 19–28
30. Gallego del Sol, F., and Marina, A. (2013) Structural basis of Rap phosphatase inhibition by Phr peptides. *PLoS Biol.* **11,** e1001511
31. Parashar, V., Jeffrey, P. D., and Neiditch, M. B. (2013) Conformational change-induced repeat domain expansion regulates Rap phosphatase quorum-sensing signal receptors. *PLoS Biol.* **11,** e1001512
32. Schöbel, S., Zellmeier, S., Schumann, W., and Wiegert, T. (2004) The *Bacillus subtilis* σW anti-σ factor RsiW is degraded by intramembrane proteolysis through YluC. *Mol. Microbiol.* **52,** 1091–1105
33. Zellmeier, S., Schumann, W., and Wiegert, T. (2006) Involvement of Clp protease activity in modulating the *Bacillus subtilis* σ w stress response. *Mol. Microbiol.* **61,** 1569–1582
34. Busso, D., Delagoutte-Busso, B., and Moras, D. (2005) Construction of a set Gateway-based destination vectors for high-throughput cloning and expression screening in *Escherichia coli*. *Anal. Biochem.* **343,** 313–321